J. Membrane Biol. 195, 73–84 (2003)
DOI: 10.1007/s00232-003-2046-4

The Journal of
Membrane
Biology

© Springer-Verlag New York Inc. 2003

Cl^- Channels in Basolateral TAL Membranes. XIX. Cytosolic Cl^- Regulates mmClC-Ka and mcClC-Ka Channels

C.J. Winters, M.V. Mikhailova, T.E. Andreoli
Division of Nephrology, Department of Internal Medicine, University of Arkansas College of Medicine, and The Central Arkansas Veterans Healthcare System, Little Rock, Arkansas, USA

Received: 5 February 2003/Revised: 28 June 2003

Abstract. We evaluated the effects of culturing mouse MTAL cells under conditions that suppressed steady-state cytosolic Cl^- on chloride channels fused into bilayers from basolateral vesicles of cultured MTAL cells. We used two agents to suppress Cl^- entry: 10^{-6} M PGE_2 and 10^{-4} M bumetanide. Basolateral Cl^- channels from control cultured MTAL cells exhibited the signature characteristics of mmClC-Ka channels: increased open-time probability (P_o) either by raising cytosolic-face [Cl^-] or, at 2 mM cytosolic Cl^-, by adding (ATP + PKA), and first-order conductance kinetics. Either 10^{-6} M PGE_2 or 10^{-4} M bumetanide in culture media reduced steady-state MTAL cytosolic Cl^-. Chloride channels from these cells exhibited characteristics unique to CTAL mcClC-Ka channels, namely: no augmentation of P_o either by raising cytosolic Cl^- or with cytosolic (ATP + PKA), and multi-ion occupancy. Semi-quantitative RT-PCR and real-time quantitative PCR showed that culturing MTAL cells with 10^{-6} M PGE_2 or 10^{-4} M bumetanide reduced mRNA levels encoding mmClC-Ka but not mRNA levels encoding mcClC-Ka. However, when MTAL cells were cultured under control conditions, and then pre-incubated for 60 minutes with 10^{-4} M bumetanide, cytosolic Cl^- fell acutely but Cl^- channels exhibited characteristics of mmClC-Ka channels. Thus PGE_2 and bumetanide, both of which lower steady-state MTAL cytosolic Cl^- concentrations, inhibit either the transcriptional and/or the translational processes for mmClC-Ka synthesis.

Key words: Cl^- Channels — MTAL — mmClC-Ka — mcClC-Ka

Correspondence to: T.E. Andreoli; email: AndreoliThomasE@uams.edu

Introduction

This paper reports the effects of culturing mouse MTAL cells under conditions that reduce cytosolic Cl^- concentrations in growing cells on the functional activity of two basolateral Cl^- channels, mmClC-Ka and mcClC-Ka, obtained from MTAL cells. Cultured mouse MTAL cells contain the two highly homologous mRNAs encoding the Cl^- channels mmClC-Ka and mcClC-Ka [15]. Under normal growth conditions [20, 33, 34, 40], Cl^- channels fused into bilayers from basolateral membrane vesicles of cultured mouse MTAL cells exhibit the typical functional characteristics of mmClC-Ka channels, namely: an increase in the open time probability (P_o) with elevations of cytosolic-face Cl^- concentrations ($K_{1/2}$ = 10 mM Cl^- [20, 29–31, 40]); an increase in P_o when cytosolic faces are exposed to (ATP + PKA) at 2 mM cytosolic-face Cl^- [20, 29, 30, 40]; and first-order kinetics of ion conductance typical of single-ion channel occupancy [12, 13, 34].

In the preceding paper [37], we showed that, when Cl^- channels were fused into bilayers from basolateral MTAL vesicles, cytosolic-face addition of phenylglyoxal (PGO), which presumably blocks Cl^- interaction by covalent binding to arginine or lysine residues [14, 23, 24, 31], altered the properties of mmClC-Ka channels to those characteristic of mcClC-Ka channels [33, 36, 40], namely: no increase in P_o when raising cytosolic-face Cl^- concentrations from 2 mM to 50 mM; no increase in P_o when (ATP + PKA) were added to cytosolic-face Cl^- concentrations at 2 mM cytosolic face Cl^-; and self-block kinetics of ion conductance typical of multi-ion occupancy. These properties were previously observed only in Cl^- channels from cultured CTAL cells [33, 36, 40].

To explore further the relations between cellular Cl^- concentrations and basolateral Cl^--channel

functional activity in cultured mouse MTAL cells, we cultured the latter under three sets of conditions: control circumstances [15, 33, 34]; in the presence of 10^{-6} M PGE_2, which suppresses adenylate cyclase activation of $Na^+/K^+/2Cl^-$ entry in microperfused mouse MTAL segments by activating G_i, the guanine nucleotide regulatory subunit that inhibits activity of the catalytic subunit of adenylate cyclase [3, 4, 22]; and in the presence of 10^{-4} M bumetanide, which inhibits $Na^+/K^+/2Cl^-$ entry into cultured MTAL cells or microperfused MTAL or CTAL segments [9, 10, 16, 21]. We found that, either with PGE_2 or bumetanide addition to the culture media, the MTAL cells had significantly lower steady-state cytosolic Cl^- concentrations than control cells.

Chloride channels from basolateral membranes of control MTAL cells, when fused into bilayers, had the signature properties of mmClC-Ka channels. However, Cl^- channels fused into bilayers from MTAL cells grown in the presence of either PGE_2 or bumetanide had the characteristic properties of mcClC-Ka channels. Furthermore, using either semiquantitative RT-PCR or real-time quantitative PCR, we found that cultured MTAL cells grown in the presence of PGE_2 or bumetanide had dramatically reduced levels of the DNA fragment specific for mmClC-Ka, while there was no detectable change in the levels of the DNA fragment specific for mcClC-Ka. Finally, control MTAL cells pre-incubated for one hour with bumetanide yielded Cl^- channels which, when fused into bilayers, had the typical properties of mmClC-Ka channels, despite the fact that the one hour pre-incubation of control MTAL cells with 10^{-4} M bumetanide also reduced strikingly cytosolic Cl^- concentrations. Thus we conclude that, in these cultured MTAL cells, steady-state reductions in cytosolic Cl^- concentrations suppressed gene transcription and/or mRNA translation responsible for encoding mmClC-Ka.

Preliminary reports of these findings have appeared in abstract form [38, 39].

Materials and Methods

The mouse MTAL and CTAL cells used in the present studies were identical to those described in the previous paper [37] and in earlier publications [20, 33, 34, 40].

Measurement of Cytosolic Cl^- Concentrations

Mouse CTAL and MTAL cells were grown to confluence on Corning 75-cm tissue culture flasks in a 1:1 mixture of Dulbecco's Modified Eagle's Medium and Ham's F12 Nutrient Mix plus 5% fetal bovine serum with penicillin G (100 units/mL), streptomycin sulfate (100 μg/ml) and 15 mM HEPES (pH 7.4). Where indicated, either 1 μM PGE_2 or 0.1 mM bumetanide was added to the growth medium in paired experiments. In a separate set of paired experiments, MTAL cells were pre-incubated for 1 hour with an ADH cocktail containing 0.2 μU/mL ADH, 20 μM forskolin and 0.5 mM db-cAMP [15, 33], either without or with 0.1 mM bumetanide in the pre-incubation media. Similarly, CTAL cells were pre-incubated for 1 hour either with or without 0.1 mM bumetanide or 1 μM PGE_2.

In all experiments, the cells were gently removed from flasks by scraping, isolated by centrifugation (800 × g) and washed in a 250 mM sucrose/30 mM histidine (pH 7.4) HS buffer. The cells were again isolated by centrifugation (800 × g), HS buffer removed and the resultant pellets sonicated with a Virsonic 475 pulse sonicator (Virtis Company, Gardiner, NY). Intracellular Cl^- concentrations were measured as described by Cotlove, et al. [1, 2], using a Buchler Digital Chloridometer model 4-2500 (Buchler Instruments, Fort Lee, NJ); that is, total chloride ion content was measured in 100-μL aliquots of sonicated cells. The chloridometer was standardized using control chloride solutions and was linear over the range of 5 mM to 100 mM ($X = 0.97y + 0.10$, $R = 0.997$).

Semiquantitative RT-PCR Analysis

Semiquantitative RT-PCR analysis [5, 17, 18, 25] using poly(A) + mRNA from MTAL cells and primers specific for either the cDNA *mmClC-Ka*, which encodes mmClC-Ka, or for cDNA *mcClC-Ka*, which encodes mcClC-Ka, was carried out on cultured mouse MTAL cells as described in detail previously [15]. As in the latter study, measurements were considered reliable when the RT-PCR product DNA fragment accumulation was in the linear range, that is, 5–50 ng DNA/sample and 15–25 cycles. Thus, in the experiments reported in Fig. 8, the dashed line indicates the lower limit for linear RT-PCR DNA fragment accumulation. Beta-actin control RT-PCR experiments carried out contemporaneously with these studies are shown in Figs. 7 and 8. As indicated in Figs. 7 and 8, the control β-actin experiments yielded predicted DNA fragments 400 base pairs in length, a result identical to that observed in our prior studies [15].

In the experiments reported in Figs. 7 and 8, cultured mouse MTAL cells were grown in paired experiments with and without 1 μM PGE_2 in the growth medium, and RT-PCR DNA fragment levels were measured at the same cell passage for both control and PGE_2-treated cells. As in our prior studies [15], PCR reactions were performed using a Gene-Amp PCR System 9600 (Perkin-Elmer), the products were separated on 1% agarose gels and visualized by ethidium-bromide staining. The relative band intensities corresponding to PCR products of expected molecular mass were quantified by a densitometer (Eagle Eye II; Stratagene, La Jolla, CA) using a 100 bp Mass Standard (New England Biolabs, Beverly, MA).

Real-Time Quantitative PCR

RNA was isolated from MTAL cells using a FastTrack 2.0 Kit (Invitrogen, Carlsbad, CA) and quantified by spectrophotometry. RNA was transcribed using reverse transcriptase from Gene AMP Gold RNA PCR Core Kit (PE Biosystems, Foster City, CA) as described previously [15]. For quantification of *mmClC-Ka* and *mcClC-Ka* gene expression, quantitative PCR with internal fluorescent hybridization probes in the ABI Prism 7700 sequence detection system was used.

Primers and probes for PCR were designed based on sequence differences between *mmClC-Ka* and *mcClC-Ka* [15]. The upstream PCR primer 5′-TGA-GCT-GGT-ACA-ACT-ACA-3′ for *mmClC-Ka* corresponded to the region from base 924 to base 945 (bases are numbered as for the sequence with GenBank accession number AF124847), and the reverse primer 5′-GGT-TTG-CTG-GTA-

GCC-AG-3′ corresponded to the region from base 999 to base 1015. The upstream PCR primer 5′-TTT-ACC-TGT-TCT-GTC-AGC-GAA-ATT-3′ for *mcClC-Ka* corresponded to the region from base 1041 to base 1064 (bases are numbered as for the sequence with GenBank accession number AF124848), and the reverse primer 5′-CGT-AGG-ACG-GCT-TGC-TTG-TAG-3′ corresponded to the region from base 1125 to base 1145. The internal oligonucleotide probe was labeled with the fluorescent dyes 5-carboxyfluoroscein (FAM) on the 5′ end and N,N,N′,N′-tetramethyl-6-carboxyrhodamine (TAMRA) on the 3′ end. The internal *mmClC-Ka* TaqMan probe (Synthegen, Houston, TX) was hybridized within the 91-bp region amplified by the *mmClC-Ka* PCR primers and had a sequence 5′-(FAM)-CTT-ATT-TTT-CCT-CAA-GGC-CAA-TGG GTT-(TAMRA)-3′. The internal mcClC-Ka TaqMan probe was hybridized within the 90-bp region amplified by the mcClC-Ka PCR primers and had a sequence 5'-(FAM)-TCT-CCG-CTT-CAT CAA-GAC-CAA-TCG-CTA-(TAMRA)-3′. This combination of primers and probes provided no cross reactivity as detected in control experiments, and had no homology with other sequences in GenBank.

The TAMRA emission spectrum was used to standardize for background fluorescence [11, 26]. The quantity of DNA and cDNA in each reaction was determined with reference to a standard curve generated by amplification of known amounts of target DNA or RNA (converted to cDNA). As reported for the DNA TaqMan assay [6], the standard curves for the RNA targets were linear over 5 orders of magnitude, with an intra- or interassay coefficient of variation of less than 10% with standards.

The PCR mixture (50 μl total volume) consisted of *mmClC-Ka* or *mcClC-Ka* upstream and reverse primers 0.8 μM each, 100 nM TaqMan probe, dATP, dCTP and dGTP (Pharmacia, Alameda, CA) each at a concentration of 200 nM, 400 nM dUTP (Pharmacia), 5 mM $MgCl_2$, 100 ng of bovine serum albumin per μL (Pharmacia), 10 ng of yeast RNA (Ambion) per μL, 1 U of uracil DNA glycosylase (New England Biolabs, Beverly, MA), 1 U of *Taq* polymerase (Invitrogen), and PCR buffer (20 mM Tris-HCl, pH 8.4, 50 mM KCl). Amplification and detection were performed with the ABI 7700 system utilizing the following profile: 1 cycle of 50°C for 2 min, 1 cycle of 95°C for 5 min, 40 cycles of 94°C for 30 sec, and 60°C for 1 min for mmClC-Ka or 62°C for mcClC-Ka for 1 min.

The threshold was set at 10 times the standard deviation of the mean baseline emission calculated for PCR cycles 3 to 10. The fractional cycle number reflecting a positive PCR result is called the cycle threshold (*Ct*). The *Ct* values for standards and samples were usually in the range of between 18 and 32 cycles of amplification. The amount of product in a particular reaction mixture was measured by interpolation from a standard curve of *Ct* values generated from known starting concentrations of DNA. The efficiency of each RT reaction was determined by the use of in vitro-transcribed RNA from the cloned *mmClC-Ka* and *mcClC-Ka* genes. Dilutions of control transcripts ranging to 10^2 to 10^5 molecules μL^{-1} in 10 ng μL^{-1} yeast carrier RNA (Ambion) were included in each RT-PCR assay. RT assays of markedly low efficiency (< 0.5%) were rejected and repeated. To estimate possible DNA contamination, all samples were subject to a no-RT control which was then subtracted from the RNA result. All RT reactions were also controlled by blank samples with and without RT enzyme.

$^{36}Cl^-$ Fluxes in Cultured Mouse MTAL Cells

The $^{36}Cl^-$-uptake experiments were carried out by rapid filtration using Millipore filters (HAWP pore size 0.45 μm) as described previously [32, 35]. MTAL cells were suspended in a HEPES buffered salt solution (HBS) containing (mM): 135 NaCl, 5 KCl, 1 $MgCl_2$, 1 $CaCl_2$, 10 glucose, 10 HEPES and 1 NaH_2PO_4 (pH 7.4) for 15 min. prior to assay at 37°C. When present, ADH cocktail and/or 1 μM PGE_2 were added 15 min. prior to assay. $^{36}Cl^-$ uptake was initiated by the addition of $^{36}Cl^-$ at a final concentration of 4.5 mM. Aliquots of 100 μL of the reaction mixtures were applied to the filters at timed intervals and washed to terminate $^{36}Cl^-$ uptake.

$^{36}Cl^-$ Efflux

The $^{36}Cl^-$ effluxes were carried out as described previously [35]. In paired experiments, MTAL cells were grown to confluence on 6-well cell culture plates. The latter contained either: control medium; control medium with 1 μM PGE_2; or control medium with 10^{-4} M bumetanide. The cells were loaded with 1 μC/mL $^{36}Cl^-$ for 12 hours. Where indicated, ADH cocktail was pre-incubated for 1 hour with the cells. The cells were then washed 3 times with 2 mL of HBS and efflux was measured by removing and replacing the buffer at timed intervals up to 10 min. Rate constants were derived by fitting the data to first-order exponential decay using Origin 4.1 (Microcal Software, Northhampton, MA) and expressed as $T_{1/2}$.

Single-channel Recordings in Planar Lipid Bilayers

The procedures for preparing basolaterally-enriched vesicles from cultured mouse MTAL or CTAL cells have been described in detail elsewhere [20, 33, 34, 40] and were utilized in identical fashion in the present studies. Likewise, the techniques for forming lipid bilayers and for measuring the electrical properties of Cl^- channels incorporated into bilayers were the same as those used in the preceding paper [37] and in earlier studies [19, 20, 28, 33, 34]. In all cases, experimental data were expressed as mean values ± SEM for the indicated number of experiments. A single bilayer was taken to be $n = 1$. Curve fitting and simple linear regression were done on computer using Origin 4.1 (Microcal Software).

Results

Cytosolic Cl^- Concentrations for Various Culture Media or Pre-incubation Conditions

Table 1 shows the results of two different sets of paired experiments examining cytosolic Cl^- concentrations under different conditions. In the first set, MTAL cells were grown under control conditions using the medium typically used for cell culture in our laboratory (Methods; [20, 33, 34, 40]) and, contemporaneously, either with 10^{-6} M PGE_2 or with 10^{-4} M bumetanide addition to the culture medium. PGE_2 was chosen because, in microperfused MTAL segments, PGE_2 blocks ADH- or db-cAMP-mediated enhancement of net Cl^- absorption by activating the G_i guanine nucleotide regulatory subunit of adenylate cyclase, thus suppressing activity of the latter [3, 4, 22]. And to insure that the observed PGE_2 effects were not referable to other, undefined actions of PGE_2 on growing MTAL cells in culture, we carried out parallel experiments using 10^{-4} M bumetanide addition to the culture medium, since bumetanide is a specific blocker of $Na^+/K^+/2Cl^-$ entry across apical membranes in cultured mouse MTAL cells [9, 10, 16].

Table 1. Effects of various pre-incubation conditions or additions to growth medium on intracellular [Cl^-] in cultured mouse MTAL cells

One-hour pre-incubation	Growth medium	Intracellular [Cl^-] (mM)	n	P
None	control	19.4 ± 0.4	9	–
None	1 μM PGE_2	11.3 ± 1.5	6	0.0002
None	0.1 mM bumetanide	7.7 ± 1.2	6	0.000002
ADH cocktail	Control	25.3 ± 0.7	4	0.002
0.1 mM bumetanide	Control	9.5 ± 1.2	4	0.001

MTAL cells were cultured contemporaneously using the culture conditions described previously [20, 32, 35]. In paired culture experiments, either 1 μM PGE_2 or 0.1 mM bumetanide was added to the control culture medium. In the paired pre-incubation experiments, the ADH cocktail, when present, contained 0.2 μU/ml ADH, 20 μM forskolin and 0.5 mM db-cAMP (*see* Ref. 32). All p values are referable to the experiments without pre-incubation and using control growth medium.

Table 2. The effect of PGE_2 in growth medium on the $T_{1/2}$ for $^{36}Cl^-$ efflux in cultured mouse MTAL cells

Growth medium	Control $T_{1/2}$		ADH-cocktail $T_{1/2}$
		(sec)	
Control	158 ± 7	——— (n = 6; p = 0.00001) ———	94 ± 3
	N.S.		p = 0.00001
Control + 10^{-6} M PGE_2	143 ± 6	——— (n = 6; p = NS) ———	145 ± 5

Paired experiments in which MTAL cells were cultured either under control conditions [20, 32, 35] for cell culture or with control medium to which was added 10^{-6} M PGE_2. The cells were loaded with $^{36}Cl^-$ as described previously [32, 35] and the $T_{1/2}$ for $^{36}Cl^-$ efflux was measured, in paired experiments, as described previously [35]. The incubation media for $^{36}Cl^-$ efflux experiments were either control solution, control solution to which was added 10^{-6} M PGE_2 with or without an ADH cocktail, which included 0.2 μU/mL vasopressin, 20 μM forskolin and 0.5 mM db-cAMP, as in our prior experiments [32].

Table 3. Effect of PGE_2 pre-incubation on initial rates of $^{36}Cl^-$ uptake in cultured mouse MTAL cells

One-hour pre-incubation	$^{36}Cl^-$ uptake (mM/mg protein · 30 sec)	n	p
None	42.8 ± 13.2	5	0.04
ADH cocktail	111.6 ± 41.1	5	0.004
ADH cocktail 1 μM PGE_2	17.4 ± 7.5	5	

Cultured mouse MTAL cells were pre-incubated under the indicated conditions (*see* Table 1). The p values compare the control values withthose with pre-incubation using the ADH cocktail, and pre-incubation with ADH cocktail either with or without 1 μM PGE_2.

The results presented in Table 1 show clearly that, either with PGE_2 or bumetanide addition to the culture medium, cultured MTAL cells had significantly lower cytosolic Cl^- concentrations than cells cultured under control conditions.

In the second set of paired experiments, we evaluated the effects of pre-incubating MTAL cells grown under control conditions for one hour either with an ADH cocktail or with bumetanide. In keeping with earlier studies from this [9, 10, 16] and other laboratories [21] on microperfused MTAL segments, the ADH cocktail increased significantly cytosolic Cl^- concentrations from 19.4 ± 0.4 mM to 25.3 ± 0.7 mM. Furthermore, one hour pre-incubation of the control cells with bumetanide produced the expected fall in cytosolic Cl^- concentrations.

In prior studies [32, 35], we found that, in cultured MTAL but not CTAL cells, activation of the adenylate cyclase cascade augmented the rates of bumetanide-sensitive $^{36}Cl^-$ uptake and bumetanide-sensitive $^{36}Cl^-$ efflux. These findings are obviously in concert with the effects of ADH or db-cAMP on enhancing net Cl^- absorption in microperfused MTAL but not CTAL segments [8, 9]. The experiments reported in Table 2 examined the effects of adding PGE_2 to the growth medium on the $T_{1/2}$ for $^{36}Cl^-$ efflux in MTAL cells. In keeping with our earlier findings [32, 35], control cells incubated with the ADH cocktail had a considerably shorter $T_{1/2}$ for $^{36}Cl^-$ efflux than control cells. However, the addition of PGE_2 to culture medium abolished this ADH-dependent enhancement of the $T_{1/2}$ for $^{36}Cl^-$ efflux.

Furthermore, as indicated in Table 3, pre-incubation of control cells with an ADH cocktail increased significantly the rate of $^{36}Cl^-$ uptake, a finding in keeping with our prior studies [32, 35]. Of particular pertinence to the present studies, the results in Table 3 also show that PGE_2 suppressed dramatically both the control and the ADH-stimulated rates of $^{36}Cl^-$ uptake. Thus, when considered together, the data in Tables 1–3 indicate that, in accord with findings in microperfused MTAL segments [3, 4], PGE_2 sup-

Table 4. Effects of various additions to growth medium on intracellular [Cl^-] in cultured mouse MTAL and CTAL cells

Cells	Growth medium	Intracellular [Cl^-] (mM)	*n*	*p*	*p*
MTAL	Control	19.4 ± 0.9	9	–	
CTAL	Control	13.5 ± 0.5	11	0.00002	–
CTAL	Control + 1 μM PGE_2	12.0 ± 0.8	11		>0.1
CTAL	Control + 0.1 mM bumetanide	8.4 ± 0.8	8		0.00003

MTAL and CTAL cells were cultured as described previously [20, 33, 34]. In paired culture experiments with CTAL cells, either 1 μM PGE_2 or 0.1 mM bumetanide was added to the culture medium. The *p* values compare either control CTAL cells with control MTAL cells; or CTAL cells grown with either PGE_2 or bumetanide in culture medium to control CTAL cells grown under control conditions.

pressed the rate of Cl^- entry and the rate of Cl^- efflux from MTAL cells. Moreover, the suppression of Cl^- entry when PGE_2 was added to culture medium also resulted in a significant reduction of cytosolic Cl^- concentration with respect to MTAL cells grown under control conditions.

Finally, ADH enhances net Cl^- absorption in microperfused MTAL but not CTAL segments [8–10, 16, 21]. Thus, in the experiments listed in Table 4, we compared cytosolic Cl^- concentrations in contemporaneously cultured MTAL and CTAL cells, as well as the effects of culturing CTAL cells either under control conditions or, in paired experiments, with 10^{-6} M PGE_2 or 10^{-4} M bumetanide in the culture medium. Three key results are evident. First, the control MTAL cells had approximately 50% greater cytosolic Cl^- concentrations than control CTAL cells. Second, in keeping with earlier data indicating that net Cl^- absorption in microperfused CTAL segments was not augmented either by ADH or by db-cAMP [3, 4, 8], the results in Table 4 show that PGE_2 addition to the culture medium had no effect on cytosolic Cl^- concentrations in CTAL cells. This finding is also consistent with the fact that adenylate cyclase activation enhances both the rate of net Cl^- uptake and the rate of net Cl^- efflux in cultured MTAL cells, while no such adenylate-cyclase effect occurs in cultured CTAL cells (Tables 2, 3; [33]). Finally, the results in Table 4 show that, in paired experiments, bumetanide addition to culture medium significantly reduced cytosolic Cl^- concentrations in CTAL cells.

Effects of 10^{-6} M PGE_2 or 10^{-4} M Bumetanide Addition to Growth Medium on Channel Characteristics

Figures. 1–6 show the effects of paired experiments assessing the effects of adding either 10^{-6} M PGE_2 or 10^{-4} M bumetanide to the culture medium on the characteristics of Cl^- channels fused into bilayers from basolateral vesicles of cultured MTAL cells. Figures 1 and 2 show paired experiments where we tested the response of Cl^- channels either to raising cytosolic-face Cl^- concentrations from 2 mM to 50 mM or, at 2 mM cytosolic-face Cl^-, adding (ATP + PKA) to cytosolic-face solutions.

The control data in the upper panel of Fig. 1 show that, when MTAL cells were grown under control conditions, the Cl^- channels exhibited the unique signature characteristics of mmClC-Ka channels [29, 31, 33], namely: a rise in P_o when cytosolic-face Cl^- concentrations were raised from 2 mM to 50 mM; and, at 2 mM cytosolic-face Cl^-, an (ATP + PKA)-mediated rise in P_o. The lower panel in Fig. 1 shows clearly that neither maneuver augmented P_o in Cl^- channels fused into bilayers from MTAL cells grown in the presence of 10^{-6} M PGE_2. Likewise, the paired data presented in Fig. 2 indicate that, when the MTAL cells were grown in the presence of 10^{-4} M bumetanide, Cl^- channels fused into bilayers from basolateral vesicles of these cells exhibited no increase in P_o either when cytosolic-face Cl^- concentrations were raised from 2 mM to 50 mM or, with 2 mM cytosolic-face Cl^-, when (ATP + PKA) were added to cytosolic-face solutions.

Figures 3–6 show paired experiments, which examined the effects of adding either 10^{-6} M PGE_2 (Figs. 3, 4) or 10^{-4} M bumetanide (Figs. 5, 6) to culture media on the kinetic properties of Cl^- channels fused into bilayers from basolateral vesicles of cultured MTAL cells. The control data presented in Figs. 3 and 4 show that, without PGE_2 or bumetanide addition to culture medium, the Cl^- channels exhibited the first-order single-occupancy kinetics typical of mmClC-Ka channels [34]. However, when the MTAL cells were grown either in the presence of PGE_2 (Figs. 3, 4) or bumetanide (Figs. 5, 6), the Cl^- channels derived from MTAL cells exhibited self-block with Hill plots typical of multi-ion occupancy and previously seen only in mcClC-Ka channels obtained from cultured CTAL cells [36] or, as noted in the preceding paper [37], in mmClC-Ka channels from MTAL cells exposed to cytosolic-face PGO after fusion into bilayers.

In short, when the MTAL cells were grown in the presence of either PGE_2 or bumetanide, each of which lowered cytosolic Cl^- (Table 1), although by different mechanisms [3, 4, 9, 10, 16, 21], the Cl^- channels derived from basolateral membranes of

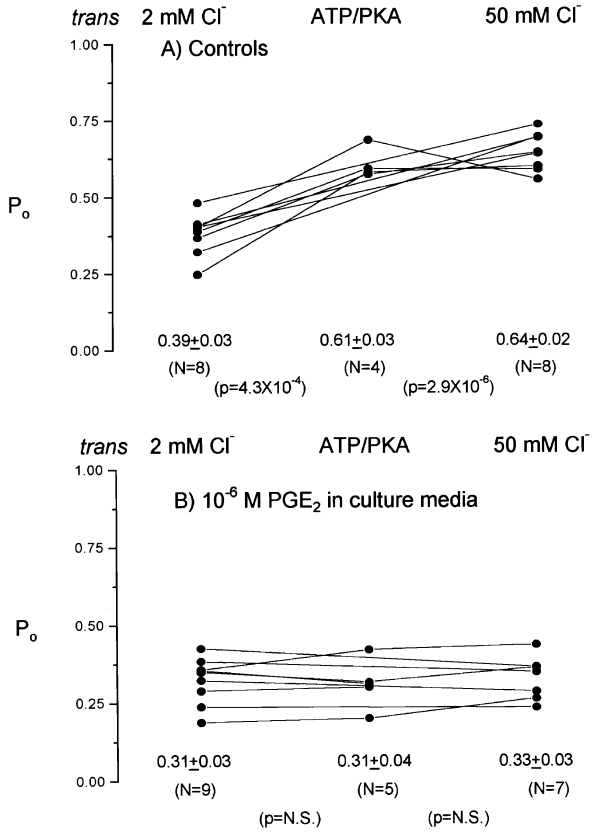

Fig. 1. Paired experiments comparing MTAL cells grown in control medium to MTAL cells cultured with 10^{-6} M PGE_2 in the growth medium on the response of Cl^- channels from basolateral vesicles fused into bilayers to variations in cytosolic-face [Cl^-] concentrations and/or (ATP + PKA). The *p* values with (ATP + PKA) and/or 50 mM Cl^- are expressed with respect to data obtained with 2 mM *trans* Cl^-.

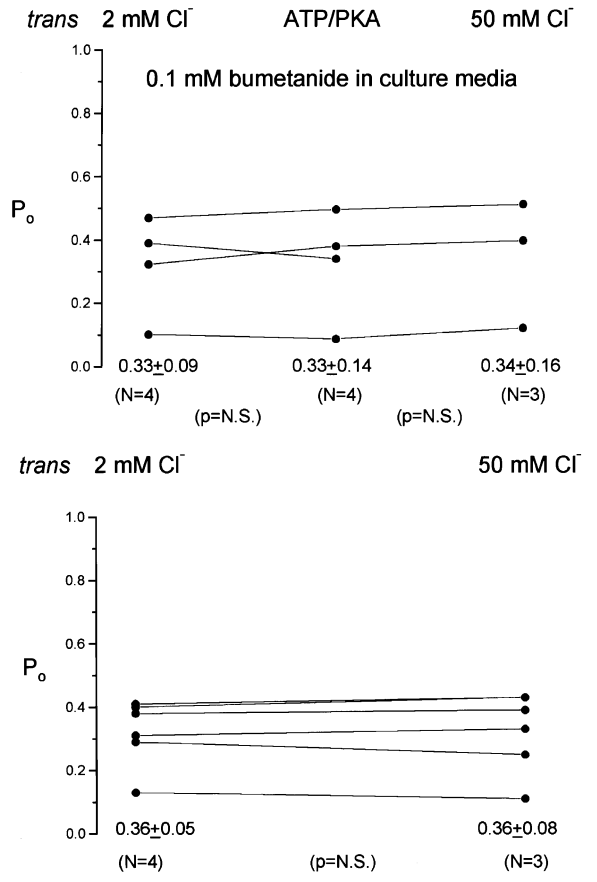

Fig. 2. Paired experiments illustrating the effects of adding 0.1 mM bumetanide to the culture medium for growing MTAL cells on the response of Cl^- channels from MTAL basolateral membrane vesicles incorporated into bilayers on variations in cytosolic-face Cl^- concentrations and/or cytoplasmic-face ATP/PKA addition. The paired control data are in the upper panel of Fig. 1. The *p* values with (ATP + PKA) and/or 50 mM Cl^- are expressed with respect to data obtained with 2 mM trans Cl^-.

those Cl^--depleted MTAL cells exhibited the properties typical of mcClC-Ka channels from CTAL cells [33, 36] rather than those of mmClC-Ka channels from MTAL cells [20, 29, 30, 33, 34]. More specifically, when MTAL cells were grown either in the presence of PGE_2 (Fig. 1) or bumetanide (Fig. 2), P_o was not enhanced either by raising cytosolic-face Cl^- from 2 mM to 50 mM or, at 2 mM cytosolic-face Cl^-, by adding (ATP + PKA) to cytosolic-face solutions. Furthermore, in contrast to the first-order single occupancy exhibited by Cl^- channels from control cells (Figs. 3, 4), channels from MTAL cells grown in the presence of PGE_2 (Figs. 3, 4) or bumetanide (Figs. 5, 6) exhibited self-block and Hill plots typical of multi-ion occupancy kinetics.

Effects of PGE_2 on RT-PCR DNA-Fragment Expression in Cultured MTAL Cells

In our prior RT-PCR studies [15], we found that poly(A) + mRNA from cultured MTAL cells used with primers specific either for the cDNA *mmClC-Ka*,

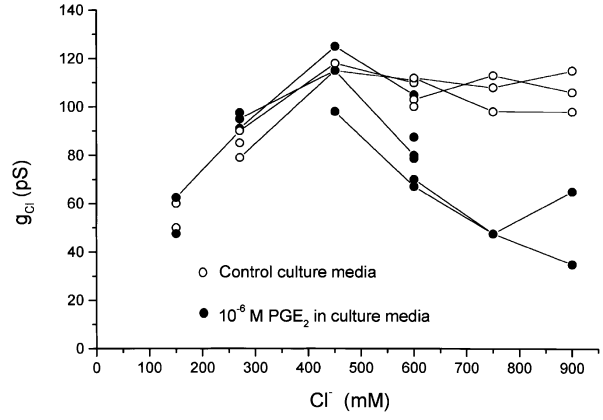

Fig. 3. Paired experiments showing the relation of g_{Cl} to symmetrical increases in external Cl^- concentrations in Cl^- channels fused into bilayers from basolateral membrane vesicles obtained from MTAL cells cultured without and with 10^{-6} M PGE_2 in the growth medium. The lines connect paired measurements in individual bilayers.

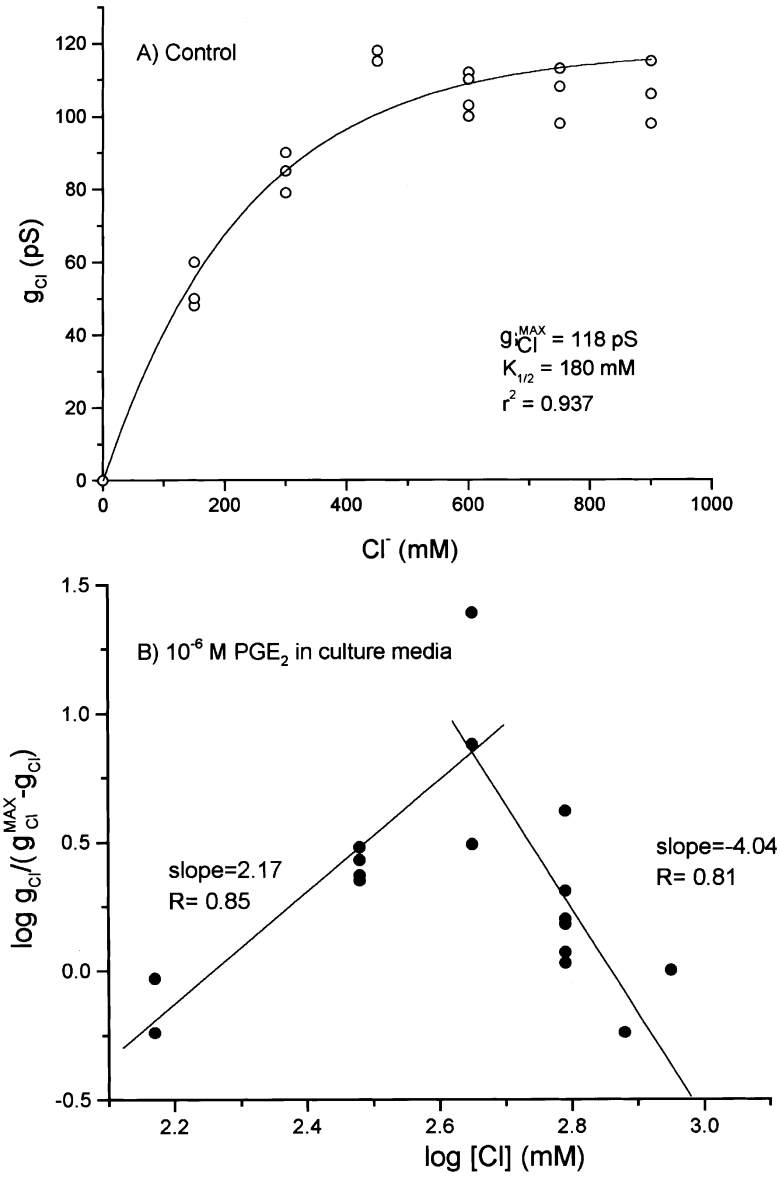

Fig. 4. A Michaelis plot of the control experiments from Fig. 3 (*upper panel*) and a Hill plot of the data from Fig. 3 (*lower panel*) with PGE_2 in the growth media. For the Hill plot, g_{Cl}^{max} was obtained, as described previously (36), from the peak g_{Cl} observed in Fig. 2.

which encodes mmClC-Ka, or for the cDNA *mcClC-Ka*, which encodes mcClC-Ka, yielded DNA fragments specific for mmClC-Ka and mcClC-Ka, respectively. In cultured mouse CTAL cells, we found RT-PCR DNA fragments encoding mcClC-Ka, and barely detectable DNA fragments encoding mmClC-Ka [15]. The results in Figs. 1–6 indicate that adding either 10^{-6} M PGE_2 or 10^{-4} M bumetanide to the growth medium for MTAL cells resulted in basolateral Cl^- channels that had the properties unique to mcClC-Ka channels typically seen in cultured CTAL cells rather than mmClC-Ka channels from MTAL cells. Accordingly, we also tested the effects of adding 10^{-6} M PGE_2 to the growth medium for culturing MTAL cells on the levels of 400 bp length DNA fragments obtained, using the same technique described previously [15], that is, using poly(A) + mRNA from cultured MTAL cells and primer specific either for *mmClC-Ka*, the gene encoding mmClC-Ka, or for *mcClC-Ka*, the gene encoding mcClC-Ka.

Figure 7 shows a representative set of RT-PCR experiments including β-actin controls and primers specific for the cDNAs *mmClC-Ka* and *mcClC-Ka*, each carried out in paired fashion using poly(A) + mRNA obtained from MTAL cells grown in the absence or presence of 10^{-6} M PGE_2. In all cases, the DNA fragments obtained had the anticipated length, 400 base pairs. Inspection of Fig. 7 shows that, when the primer was specific for *mmClC-Ka*, 10^{-6} M PGE_2 in the growth medium virtually abolished the appearance of the DNA product encoding mmClC-Ka. However, when the primer was specific for mcClC-Ka, 10^{-6} M PGE_2 in the growth medium had no

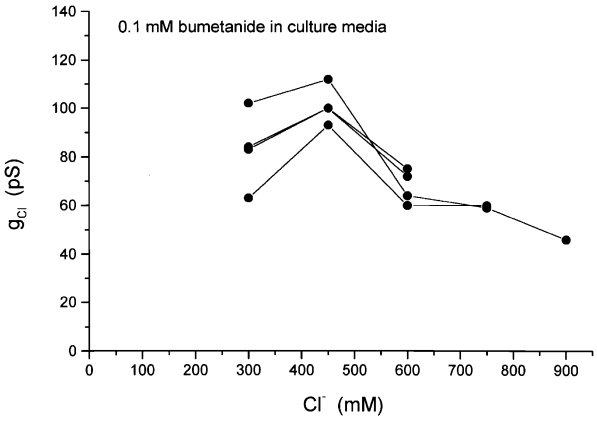

Fig. 5. Paired experiments showing the effects of adding 0.1 mM bumetanide to the growth medium for culturing MTAL cells on the variation of g_{Cl} with symmetrical increases in cis and trans Cl^- concentrations in bilayers containing Cl^- channels from basolateral membrane vesicles of MTAL cells cultured with 0.1 mM bumetanide in the growth medium. The lines connect paired measurements in individual bilayers. The control data for these experiments are shown as empty circles in Fig. 3.

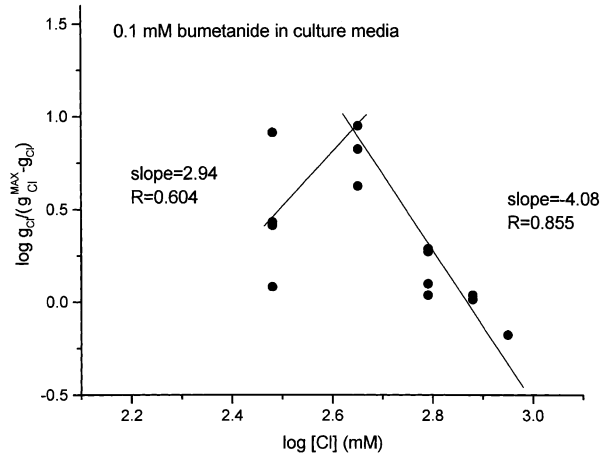

Fig. 6. A Hill plot of the data from Fig. 5. The Hill plots were carried out as described in the legend to Fig. 4.

discernible effect on the appearance of the DNA product encoding mcClC-Ka.

A complete set of semiquantitative RT-PCR results for these experiments is presented in Fig. 8. The vertical bars in Fig. 8 indicate, for these paired experiments, the mean values ± SEM of the RT-PCR products (ng/μL). The dashed horizontal line indicates the lower limit of linear RT-PCR DNA fragment accumulation, as documented in our prior studies [15]. The densitometric data illustrated in Fig. 8 show that, in cultured MTAL cells, adding PGE_2 to the growth medium had no detectable effect on the RT-PCR DNA fragment specific for encoding mcClC-Ka, 12.56 ± 2.06 ng/μL without PGE_2 and 10.96 ± 3.98 ng/μL with PGE_2 (p = N.S.). However, when PGE_2 was added to the growth medium for culturing MTAL cells, the RT-PCR DNA fragment specific for encoding mmClC-Ka was reduced from 10.77 ± 2.51 ng/μL to 4.34 ± 1.0 ng/μL (p = 0.04). Moreover, with 10^{-6} M PGE_2 in the growth medium, the RT-PCR DNA fragment of 4.34 ± 1.0 ng/μL was, as indicated in Methods, below the linear range for RT-PCR DNA fragment accumulation [15]. In short, the addition of 10^{-6} M PGE_2 to the growth medium for cultured mouse MTAL cells suppressed the RT-PCR DNA fragment specific for mmClC-Ka channels below levels detectable reliably, but had no discernible effect on the RT-PCR DNA fragment specific for encoding mcClC-Ka channels in these MTAL cells.

Real-Time Quantitative PCR

We wished to provide more stringent verification of the semiquantitative data presented in Figs. 7 and 8, and to evaluate the effects of bumetanide addition to growth medium, which also suppresses steady-state Cl^- concentrations in cultured MTAL cells (Table 1), on the mRNAs encoding mmClC-Ka and mcClC-Ka. Thus we measured, using real-time quantitative PCR ([6, 11]; Methods), *mmClC-Ka* and *mcClC-Ka* expression, using RNAs isolated from MTAL cells grown under control conditions or with either 1 μM PGE_2 or 0.1 mM bumetanide addition to the growth medium.

The results of these paired experiments are presented in Fig. 9. The data are presented as the ratios of the DNA fragments encoding either mmClC-Ka or mcClC-Ka in treated (either with bumetanide or PGE_2 in the growth medium for culturing MTAL cells) with respect to untreated (control growth medium culturing MTAL cells) MTAL cells. It is clear from the results presented in Fig. 9 that, in accord with the data presented in Figs. 7 and 8, PGE_2 addition to the growth media for culturing MTAL cells suppressed expression of the DNA fragment encoding mmClC-Ka channels by approximately 60% but did not affect expression of the DNA fragment encoding mcClC-Ka channels. Furthermore, the results presented in Fig. 9 indicate clearly that an identical pattern of results obtained using MTAL cells grown either with (Fig. 9, treated) or without (Fig. 9, untreated) bumetanide addition to the medium for culturing MTAL cells.

Effect of Pre-incubating Control MTAL Cells with Bumetanide

The results presented in Figs. 1–6 show clearly that the addition of either PGE_2 or bumetanide to the medium for culturing MTAL cells resulted in: a reduction in cytosolic Cl^- concentrations (Table 1); suppression by PGE_2 of the ADH-mediated enhancement in the $T_{1/2}$ for $^{36}Cl^-$ efflux in cultured MTAL cells (Table 2); and, for Cl^- channels fused into bilayers from MTAL cells cultured either in the presence of PGE_2 (Figs. 1, 3, 4) or bumetanide (Figs.

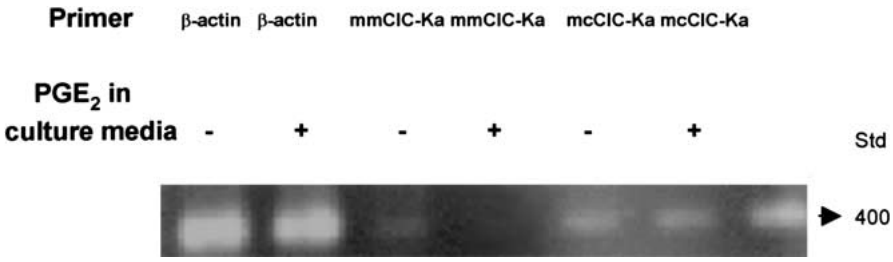

Fig. 7. A 1% agarose gel stained with ethidium bromide showing RT-PCR DNA products obtained using mRNA from MTAL cells grown with (+) and without (−) PGE_2 in the culture medium. Primers were specific for *mmClC-Ka*, *mcClC-Ka* and β-actin.

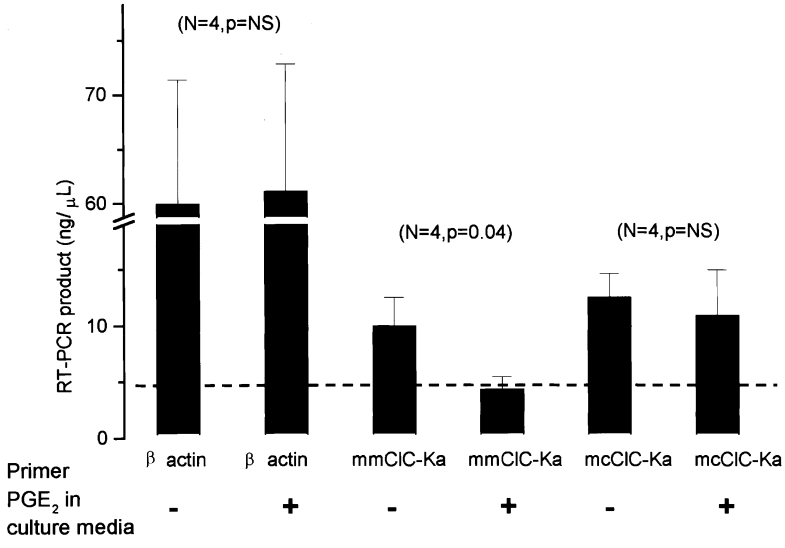

Fig. 8. Densitometric results of paired experiments illustrating the effects of 10^{-6} M PGE_2 in the growth medium for either MTAL or CTAL cells on RT-PCR DNA-fragment accumulation in cultured MTAL cells. The RT-PCR experiments were carried out using β-actin as control, as described previously [15]. The dashed line indicates the lower limit of the linear range for RT-PCR DNA-fragment accumulation of DNA fragments, determined previously in our laboratory [15].

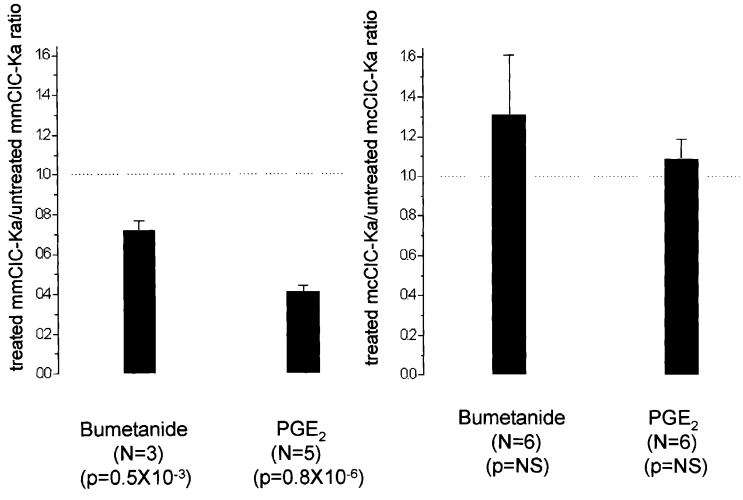

Fig. 9. The effect of bumetanide and PGE_2 on the expression of the DNA fragments encoding either mmClC-Ka or mcClC-Ka in cultured MTAL cells evaluated by real-time quantitative PCR, as described in Methods. The data are shown as the ratios of (treated) DNA fragments obtained in cells grown either in 10^{-6} M PGE_2 or 10^{-4} M bumetanide versus DNA fragments obtained from control (untreated) cells.

2, 5), Cl^- channel characteristics having the signature properties of mcClC-Ka channels derived from cultured CTAL cells [33, 36]. Since culturing MTAL cells in the presence of either PGE_2 or bumetanide resulted in a steady-state fall in cytosolic Cl^- (Table 1), it was pertinent to evaluate the effects of lowering cytosolic Cl^- concentrations acutely on the characteristics of Cl^- channels obtained from MTAL cells grown under typical conditions.

To that end, we exposed cultured MTAL cells grown under normal conditions to a one-hour pre-incubation with 10^{-4} M bumetanide. The data presented in Table 1 show that such pre-incubation reduced cytosolic Cl^- concentrations in normally cultured MTAL cells from 19.4 ± 0.4 mM to 9.5 ± 1.2 mM (p = 0.001). We then prepared basolateral vesicles from normally grown cells either pre-incubated or not pre-incubated with bumetanide and assessed the charac-

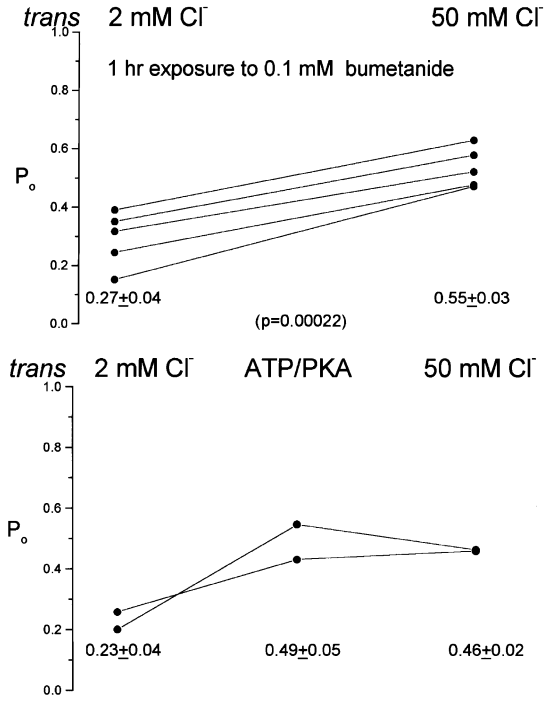

Fig. 10. The effect of exposing MTAL cells grown under control conditions (Figs. 1, 2; Table 1), then pre-incubated for 1 hour with 0.1 mM bumetanide (Table 1), on the response of Cl^-channels incorporated into bilayers from basolateral MTAL membrane vesicles, either to raising cytosolic-face Cl^- concentrations (*upper panel*) or, with 2 mM cytosolic-face Cl^-, to the sequential addition of (ATP + PKA) and 50 mM cytosolic-face Cl^-. The lines connect measurements in the same bilayers.

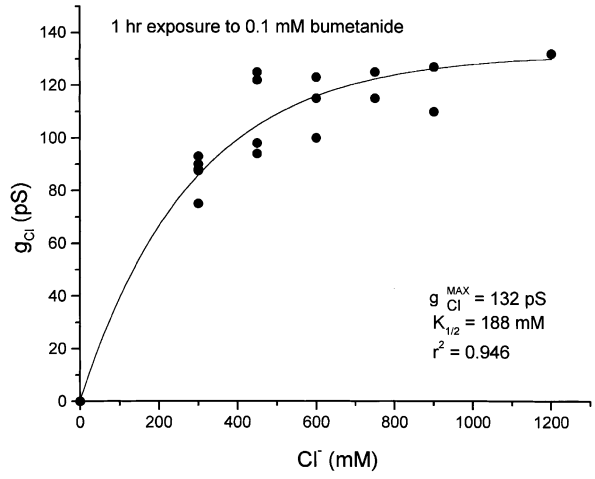

Fig. 11. A Michaelis plot of the effect of varying external Cl^- concentrations symmetrically on g_{Cl} in basolateral membrane Cl^- channels from basolateral vesicles of MTAL cells cultured under control conditions (Table 1), then exposed to 0.1 mM bumetanide for 1 hour.

teristics of Cl^- channels fused into bilayers from these two sets of vesicles.

The results of these experiments are presented in Figs. 1, 3 and 4 for Cl^- channels derived from cultured MTAL cells not pre-incubated with bumetanide, and in Figs. 10 and 11 for cultured MTAL cells pre-incubated for one hour with bumetanide. A comparison of these data shows clearly that short-term reductions in cytosolic Cl^- concentrations with bumetanide did not affect those Cl^- channel properties unique to mmClC-Ka channels, namely: augmentation of P_o by raising cytosolic-face Cl^- concentrations from 2 mM to 50 mM or, at 2 mM cytosolic-face Cl^-, by adding (ATP + PKA) to cytosolic-face solutions (Fig. 10); and first-order conductance kinetics typical of single-ion channel occupancy (Fig. 11).

Discussion

In the preceding paper [37], we found that, when basolateral vesicles from normally cultured mouse MTAL cells were incorporated into bilayers, the Cl^- channels observed when aqueous phases lacked PGO had the typical characteristics of mmClC-Ka channels [20, 29, 30, 34, 40]. However, when PGO, which binds covalently to arginine and lysine residues [14, 23, 24, 31], was added to cytosolic-face solutions, the Cl^- channel characteristics changed to those having the signature properties of mcClC-Ka channels [33, 36], and previously observed only when basolateral vesicles from cultured CTAL cells were fused into bilayers.

In order to evaluate the interactions between cytosolic Cl^- concentrations and mmClC-Ka activity, the studies reported in this paper examined, in paired experiments, the characteristics of Cl^- channels obtained from basolateral MTAL vesicles grown either under control conditions and then pre-incubated for one hour with 10^{-4} M bumetanide; or cultured with either 10^{-6} M PGE_2 or 10^{-4} M bumetanide in the growth medium. We also studied the effects of adding either 10^{-6} M PGE_2 or 0.1 mM bumetanide to growth medium on the relative abundance of the mRNAs encoding mmClC-Ka and mcClC-Ka in cultured mouse MTAL cells.

When MTAL cells were cultured in the presence of either PGE_2 or bumetanide, there was a significant drop in intracellular Cl^- (Table 1). When control MTAL cells were pre-incubated with an ADH cocktail, cytosolic Cl^- increased, while pre-incubating control MTAL cells with bumetanide significantly reduced cytosolic Cl^- (Table 1). Control MTAL cells pre-incubated with PGE_2 showed a striking inhibition of the ADH cocktail-mediated enhancement of $^{36}Cl^-$ uptake (Table 3); and culturing MTAL cells in the presence of PGE_2 suppressed the ADH-mediated enhancement in the $T_{1/2}$ for $^{36}Cl^-$ efflux (Table 2). Finally, control cultured MTAL cells had significantly higher Cl^- concentrations than control cultured CTAL cells, and PGE_2 addition to growth media had no effect on cytosolic Cl^- concentrations in cultured CTAL cells, while bumetanide addition to culture

medium reduced significantly the cytosolic Cl^- in CTAL cells. These results are consistent with earlier findings in microperfused mouse MTAL and CTAL segments, where ADH enhances apical Na^+:K^+:$2Cl^-$ entry in mouse MTAL segments [9, 10, 16] but not in mouse CTAL segments [8, 9], and PGE_2 suppresses the ADH-mediated increase in adenylate cyclase activity in microperfused MTAL segments [3, 4].

Now when the MTAL cells were cultured in the presence of either PGE_2 (Figs. 1, 3, 4) or bumetanide (Figs. 1, 5, 6), cytosolic Cl^- concentrations fell uniformly (Table 1) and the Cl^- channels fused into bilayers from basolateral vesicles of these cells uniformly exhibited the properties of mcClC-Ka channels obtained from cultured mouse CTAL cells [33, 36]. However, when control MTAL cells were pre-incubated for one hour with bumetanide, cytosolic Cl^- concentrations were also reduced significantly (Table 1), but the Cl^- channels obtained from basolateral vesicles of the control MTAL cells depleted of Cl^- by pre-incubation with bumetanide had the characteristics typical of mmClC-Ka channels (Figs. 10, 11; Refs. 20, 29–31, 34). Thus we conclude that the effects of growing MTAL cells in the presence of either PGE_2 or bumetanide, which resulted in mcClC-Ka rather than mmClC-Ka expression in bilayers (Figs. 1–6), was due to a complex mechanism initiated by steady-state reductions in cytosolic Cl^-.

In this connection, the semiquantitative RT-PCR results presented in Fig. 8 [5, 15, 17, 18, 25] and the real-time quantitative PCR results presented in Fig. 9 both indicate that, with a primer specific for *mcClC-Ka*, PGE_2 addition to the growth medium had no effect on the level of the DNA fragments that encode mcClC-Ka. However, when we used a primer specific for *mmClC-Ka*, PGE_2 addition to the growth medium suppressed the level of DNA fragments that encode mmClC-Ka below the linear range detectable for RT-PCR product accumulation. In other words, PGE_2 addition to the growth medium used to culture MTAL cells suppressed specifically the mRNA encoding mmClC-Ka but not the mRNA encoding mcClC-Ka. Moreover, the results presented in Fig. 9 also show clearly that addition of bumetanide to culture medium, which resulted in MTAL cells having significantly reduced steady-state Cl^- concentrations, and basolateral vesicles that, when fused in bilayers, had the signature characteristics of mcClC-Ka channels (Figs. 1–6), also suppressed specifically the appearance of the DNA product encoding mmClC-Ka, but not that, which encodes mcClC-Ka.

Thus it is reasonable to infer that the steady-state reductions in cytosolic Cl^-, which occurred when MTAL cells were cultured (Table 1; Figs. 1–6), with either PGE_2 or bumetanide blunted mmClC-Ka synthesis either by suppressing gene abundance and/or by inhibiting mRNA abundance encoding mmClC-Ka. The data presented in the preceding paper [37] indicate that, when basolateral MTAL vesicles are fused into bilayers, PGO addition to cytosolic-face solutions alters the properties of mmClC-Ka to channels having the conductance characteristics of mcClC-Ka channels. The mechanism for PGO inactivation of mmClC-Ka channels is not known, but it is reasonable to propose, as noted in the preceding paper [37], that inactivation may occur because covalent PGO binding to specific arginine or lysine residues on the cytoplasmic face of mmClC-Ka results in conformational changes in mmClC-Ka channels such that the latter assume the transport characteristics of mcClC-Ka channels. As noted previously [37], this argument is plausible since mmClC-Ka and mcClC-Ka channels share 95% homology.

The data presented in this paper indicate that culturing MTAL cells under conditions that lower steady-state cytosolic Cl^- concentrations—that is, with either PGE_2 or bumetanide in growth medium—inhibits either the transcriptional and/or translational events responsible for mmClC-Ka synthesis. The molecular details accounting for this inhibition of mmClC-Ka synthesis are unknown. But to our knowledge, the combined findings that pulsed increases in cytosolic-face Cl^- concentrations augment open-time probability in mmClC-Ka channels [20, 28–31, 33], while steady-state cytosolic reductions in substrate concentrations—that is, cytosolic Cl^- concentrations—suppress mmClC-Ka activity either by blocking gene expression or by reducing mRNA activity, represent a novel set of observations for ClC Cl^- channels.

We are grateful for the technical assistance provided by Ms. Anna Grace Stewart and for assistance in preparing this manuscript provided by Ms. Clementine Whitman. We also gratefully acknowledge the advice and guidance we obtained from Drs. Kathleen Eisenach, Aiwei Yao-Borengasser and Ms. Shima Patel, all from the Department of Pathology at the University of Arkansas College of Medicine, in carrying out the real-time quantitative PCR experiments illustrated in Fig. 9. This work was supported by NIH Grant 5 R01 DK25540 to T.E. Andreoli.

References

1. Cotlove, E., Trantham, H.V., Bowman, R.L. 1958. An instrument and method of automatic, rapid, accurate and sensitive titration of chloride in biological samples. *J. Lab. Clin. Med.* **51:**461–473
2. Cotlove, E. 1963. Determination of the true chloride content of biological fluids and tissues. *Anal. Chem.* **35:**95–104
3. Culpepper, R.M., Andreoli, T.E. 1983. Interactions among prostaglandin E_2 antidiuretic hormone, and cyclic adenosine monophosphate in modulating Cl^- absorption in single mouse medullary thick ascending limbs of Henle. *J. Clin. Invest.* **71:**1588–1601
4. Culpepper, R.M., Andreoli, T.E. 1984. PGE_2 forskolin and cholera toxin interactions in modulating NaCl transport in mouse mTALH. *Am. J. Physiol.* **247:**F784–F792

5. Das, S.J., Olsen, I. 2001. Up-regulation of keratinocyte growth factor and receptor: a possible mechanism of action of phenytoin in wound healing. *Biochem. Biophys. Res. Comm.* **282:**875–881
6. Desjardin, L.E., Chen, Y., Perkins, M.D., Teixeira, L., Cave, M.D., Eisenach, K.D. 1998. Comparison of the ABI 7700 system (TaqMan) and competitive PCR for quantification of IS6110 in sputum during treatment for tuberculosis. *J. Clin. Microbiol.* **36:**1964–1968
7. Dutzler, R., Campbell, E.B., Cadene, M., Chait, B.T., MacKinnon, R. 2002. X-ray structure of a ClC chloride channel at 3.0 Å reveals the molecular basis of anion selectivity. *Nature*. **415:**287–294
8. Friedman, P.A., Andreoli, T.E. 1982. CO_2-stimulated NaCl absorption in the mouse renal cortical thick ascending limb of Henle. Evidence for synchronous Na^+/H^+ and Cl^-/HCO_3^- exchange in apical plasma membranes. *J. Gen. Physiol.* **80:**683–711
9. Hebert, S.C., Culpepper, R.M., Andreoli, T.E. 1981. NaCl transport in mouse medullary thick ascending limbs. I. Functional nephron heterogeneity and ADH-stimulated NaCl cotransport. *Am. J. Physiol.* **10:**F412–F431
10. Hebert, S.C., Andreoli, T.E. 1984. Effects of antidiuretic hormone on cellular conductive pathways in mouse medullary thick ascending limbs of Henle. II. Determinants of the ADH-mediated increases in transepithelial voltage and in net Cl^- absorption. *J. Membrane Biol.* **80:**221–233
11. Heid, C.A., Stevens, J., Livak, K.J., Williams, P.M. 1996. Real time quantitative PCR. *Genome Res.* **6:**986–994
12. Hille, B. 1992. Selective permeability: saturation and binding. *In:* Ionic Channels of Excitable Membranes. pp. 362–389, Sinauer Associates, Sunderland, MA
13. Läuger, P. 1987. Dynamics of ion transport systems in membranes. *Physiol. Rev.* **67:**1196–1331
14. Lundblad, R.L. 1991. Chemical Reagents for Protein Modification. CRC Press, Boca Raton, FL
15. Mikhailova, M.V., Winters, C.J., Andreoli, T.E. 2002. Cl^- channels in basolateral TAL membranes. XVI. MTAL and CTAL cells each contain the mRNAs encoding mmClC-Ka and mcClC-Ka. *Kidney Int.* **61:**1003–1010
16. Molony, D.A., Reeves, W.B., Hebert, S.C., Andreoli, T.E. 1987. ADH increases apical Na^+:K^+:2Cl^- entry in mouse medullary thick ascending limbs of Henle. *Am. J. Physiol.* **252:**F177–F187
17. Ogretmen, B., Kraveka, J.M., Schady, D., Usta, J., Hannuny, A., Obeid, L.M. 2001. Molecular mechanisms of ceramide-mediated telomerase inhibition in the A549 human lung adenocarcinoma cell line. *J. Biol. Chem.* **276:**32506–32514
18. Ohno, J., Horio, Y., Sekido, Y., Hasegawa, Y., Takahashi, M., Nishizawa, J., Saito, H., Ishikawa, F., Shimokata, K. 2001. Telomerase activation and p53 mutations in urethane-induced A/J mouse lung tumor development. *Carcinogenesis* **22:**751–756
19. Reeves, W.B., Andreoli, T.E. 1990. Cl^- transport in basolateral renal medullary vesicles. II. Cl^- channels in planar lipid bilayers. *J. Membrane Biol.* **113:**57–65
20. Reeves, W.B., Winters, C.J., Filipovic, D.M., Andreoli, T.E. 1995. Cl^- channels in basolateral renal medullary vesicles. IX. Channels from mouse mTAL cell patches and medullary vesicles. *Am. J. Physiol.* **269:**F621–F627
21. Schlatter, E., Greger, R. 1985. cAMP increases the basolateral Cl^- conductance in the isolated perfused medullary thick ascending limb of Henle's loop of the mouse. *Pfluegers Arch.* **405:**367–376
22. Smith, W.L., Sonnenburg, W.K., Alien, M.L., Watanabe, T., Zhu, J., el-Harith, E.A. 1989. The biosynthesis and actions of prostaglandins in the renal collecting tubule and thick ascending limb. *Adv. Exp. Med. & Biol.* **259:**131–147
23. Spires, S., Begenisich, T. 1992. Modification of potassium channel kinetics by amino group reagents. *J. Gen. Physiol.* **99:**109–129
24. Takahashi, K. 1968. The reaction of phenylglyoxal with arginine residues in proteins. *J. Biol. Chem.* **243:**6171–6179
25. Tena-Sempere, M., Manna, P.R., Zhang, F.-P., Pinilla, L., Gonzalez, L.C., Dieguez, C., Huhtaniemi, I., Aguilar, E. 2001. Molecular mechanisms of leptin action in adult rat testis: potential targets for leptin-induced inhibition of steroidogenesis and pattern of leptin receptor messenger ribonucleic acid expression. *J. Endocrin.* **170:**413–423
26. Wayne, L.G. 1994. Dormancy of *Mycobacterium tuberculosis* and latency of disease. *Eur. J. Clin. Microbiol. Infect. Dis.* **13:**908–914
27. Weinreich, F., Jentsch, T.J. 2001. Pores formed by single subunits in mixed dimers of different ClC chloride channels. *J. Biol. Chem.* **276:**2347–2353
28. Winters, C.J., Reeves, W.B., Andreoli, T.E. 1990. Cl^- channels in basolateral renal medullary membranes. III. Determinants of single channel activity. *J. Membrane Biol.* **118:**269–278
29. Winters, C.J., Reeves, W.B., Andreoli, T.E. 1991. Cl^- channels in basolateral renal medullary membrane vesicles. IV. Interactions of Cl^- and cAMP-dependent protein kinase with channel activity. *J. Membrane Biol.* **122:**89–95
30. Winters, C.J., Reeves, W.B., Andreoli, T.E. 1992. Cl^- channels in basolateral renal medullary vesicles: V. Comparison of basolateral mTALH Cl^- channels with apical Cl^- channels from jejunum and trachea. *J. Membrane Biol.* **128:**27–39
31. Winters, C.J., Reeves, W.B., Andreoli, T.E. 1993. Cl^- channels in basolateral renal medullary membranes: VII. Characterization of the intracellular anion binding sites. *J. Membrane Biol.* **135:**145–152
32. Winters, C.J., Zimniak, L., Reeves, W.B., Andreoli, T.E. 1997. Cl^- channels in basolateral renal medullary membranes. XII. Anti-rbClC-Ka antibody blocks MTAL Cl^- channels. *Am. J. Physiol.* **273:**F1030–F1038
33. Winters, C.J., Reeves, W.B., Andreoli, T.E. 1999. Cl^- channels in basolateral TAL membranes. XIII. Heterogeneity between basolateral MTAL and CTAL Cl^- channels. *Kidney Int.* **55:**593–601
34. Winters, C.J., Reeves, W.B., Andreoli, T.E. 1999. Cl^- channels in basolateral TAL membranes. XIV. Kinetic properties of a basolateral MTAL Cl^- channel. *Kidney Int.* **55:**1444–1449
35. Winters, C.J., Zimniak, L., Mikhailova, M.V., Reeves, W.B., Andreoli, T.E. 2000. Cl^- channels in basolateral TAL membranes. XV. Molecular heterogeneity between cortical and medullary channels. *J. Membrane Biol.* **177:**221–230
36. Winters, C.J., Andreoli, T.E. 2002. Cl^- channels in basolateral TAL membranes. XVII. Kinetic properties of mcClC-Ka, a basolateral CTAL Cl^- channel. *J. Membrane Blol.* **186:**159–164
37. Winters, C.J., Andreoli, T.E. 2003. Cl^- channels in basolateral TAL membranes. XVIII. Phenylglyoxal induces functional mcClC-Ka activity in basolateral MTAL membranes. *J. Membrane Biol.* **195:**63–71
38. Winters, C.J., Mikhailova, M.V., Andreoli, I.E. 2002. mmClC-Ka and mcClC-Ka channels are both expressed in basolateral MTAL membranes. *J. Am. Soc. Neph.* **13:**74A
39. Winters, C.J., Mikhailova, M.V., Andreoli, T.E. 2002. Growth of MTAL cells having low cytosolic Cl^- suppresses mmClC-Ka expression and enhanced mcClC-Ka expression. *J. Am. Soc. Neph.* **13:**74A
40. Zimniak, L., Winters, C.J., Reeves, W.B., Andreoli, T.E. 1996. Cl^- channels in basolateral renal medullary vesicles. XI. rbClC-Ka cDNA encodes basolateral mTAL Cl^- channels. *Am. J. Physiol.* **270:**F1066–F1072